Olabode, Olaitan; Kosunen, Marko; Unnikrishnan, Vishnu; Palomaki, Tommi; Laurila, Tomi; Halonen, Kari; Ryynanen, Jussi

A Sensor Interface for Neurochemical Signal Acquisition

Published in:
2019 IEEE 62nd International Midwest Symposium on Circuits and Systems, MWSCAS 2019

DOI:
10.1109/MWSCAS.2019.8885019

Published: 01/08/2019

Document Version
Peer-reviewed accepted author manuscript, also known as Final accepted manuscript or Post-print

Please cite the original version:
Olabode, O., Kosunen, M., Unnikrishnan, V., Palomaki, T., Laurila, T., Halonen, K., & Ryynanen, J. (2019). A Sensor Interface for Neurochemical Signal Acquisition. In *2019 IEEE 62nd International Midwest Symposium on Circuits and Systems, MWSCAS 2019* (pp. 390-393). Article 8885019 (Conference proceedings : Midwest Symposium on Circuits and Systems). IEEE. https://doi.org/10.1109/MWSCAS.2019.8885019

A Sensor Interface for Neurochemical Signal Acquisition

Olaitan Olabode*, Marko Kosunen*, Vishnu Unnikrishnan*, Tommi Palomäki**,
Tomi Laurila**, Kari Halonen* and Jussi Ryynänen*
*Department of Electronics and Nanoengineering
**Department of Electrical Engineering and Automation
Aalto University School of Electrical Engineering, Espoo, Finland
Email: olaitan.olabode@aalto.fi

***Abstract*—This paper describes the design of an integrated sensor interface for neurochemical signal acquisition. Neurochemicals undergo oxidation and reduction reactions in the presence of an action potential. Thus, knowledge of the oxidation and reduction potentials of neurochemicals is important in the neurostimulation treatment of neurological and neurodegenerative diseases. The sensor interface circuit utilizes a mixed-signal design to detect the induced current from the neurochemical, in response to an applied voltage. The circuit is fabricated in 65nm CMOS technology and supports a wide input current range of $\pm 1.2\mu$A with a current resolution of $85.4p$A, enabling detection of neurochemicals within the supported current range. Measured results with dopamine concentration of 500nMol demonstrate the ability of the sensor interface circuit to detect oxidation and reduction current peaks, indicating the release times and the required oxidation and reduction potentials for neurostimulation of the neurochemical.**

I. Introduction

In recent years, there has been an increasing interest into sensing and real-time monitoring of neurochemicals in the brain, in order to understand neurochemical signalling and its relation to neurological disorders such as Parkinson's disease, Schizophrenia, Alzeihmers and Epilepsy [1], [2]. Further, the detection of the release times and concentration levels of neurochemicals in the brain provides significant value to researchers in the fields of neuroscience and medical diagnostics, which enables an improved treatment of patients suffering from neurological disorders and neurodegenerative diseases.

Neurochemicals such as dopamine, histamine and serotonin are typically monitored with the help of potentiostats [3]. Potentiostats operate based on electrochemical transduction, which involves applying a voltage (V_{cell}) across an electrochemical cell and measuring the induced reduction-oxidation (redox) current within the cell (I_{cell}) as illustrated in Fig. 1. However, potentiostats are usually designed to have a fixed input current range which limits the neurochemical concentration levels that can be detected by the potentiostat or sensor interface circuit. It is therefore desirable to have an integrated sensor interface circuit that supports a wide input current range while maintaining good current resolution. The relationship between the applied cell voltage range and the induced current within the neurochemical cell can be measured using cyclic voltammetry technique, which shows the oxidation-reduction profile of the neurochemical. Cyclic voltammetric (CV) measurements show current peaks that correspond to the oxidation and reduction of the neurochemical. Hence, the detection of

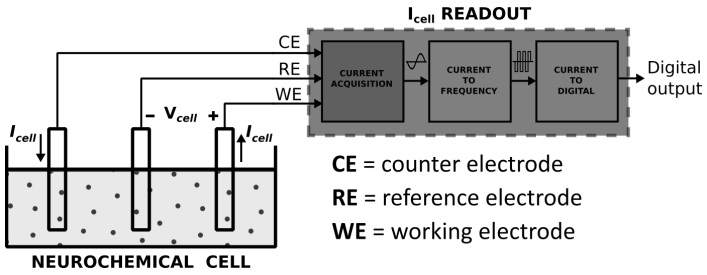

Fig. 1. System block diagram showing the neurochemical sensor electrodes and the sensor interface circuit for reading out the detected cell current.

oxidation and reduction current peaks from the sensor interface circuit can be used to estimate the release times and concentration levels of the neurochemical, which is useful in regulating medications and adjusting stimulation parameters during deep brain stimulation (DBS) treatment of patients suffering from neurological disorders such as Parkinson's disease [4].

This paper presents a sensor interface circuit that utilizes a mixed-signal design to achieve good resolution of the detected current from the neurochemical. The sensor interface circuit consists of current acquisition, current-to-frequency and current-to-digital stages as shown in Fig. 1. The sensor interface circuit is connected to the counter, reference and working electrodes (CE, RE, WE) that are inserted into the neurochemical cell, which depicts the environment in the brain. The working electrode (WE) is designed with a diamond-like carbon (DLC) material which provides good sensitivity and bio-compatibility for neurochemical sensing applications [5]. The sensor interface circuit uses a transimpedance structure in the current acquisition stage to provide the required cell voltage range of 1.5V and to support detection of a wide input current range of $\pm 1.2\mu$A. In addition, the acquired current is converted to frequency with a current-controlled oscillator (CCO) and pulses from the CCO output is used to generate digital codes in the current-to-digital stage. Measured results with dopamine concentration of 500nMol show that the circuit is able to detect oxidation-reduction current peaks and the corresponding oxidation-reduction potentials.

The rest of the paper is organized as follows. Section II describes the design of the sensor interface circuit with focus on the current acquisition process. Section III presents measured results with dopamine and the DLC electrodes. Section IV concludes the discussion.

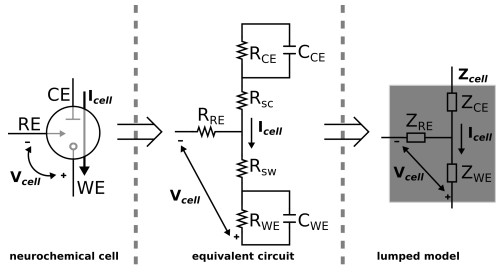

Fig. 2. Lumped impedance model of the neurochemical cell.

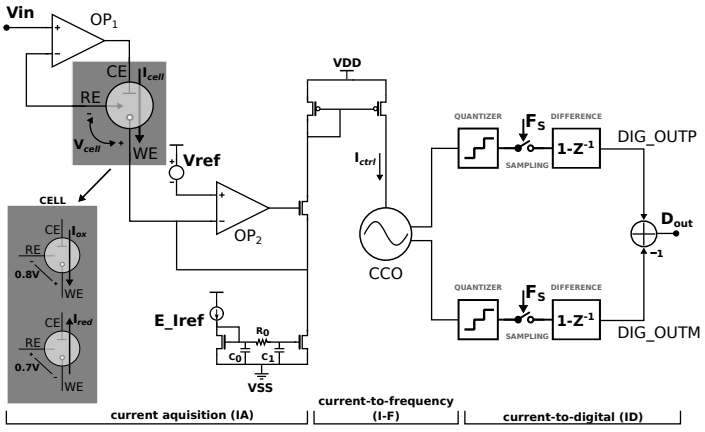

Fig. 3. Schematic of the neurochemical sensor interface circuit.

II. Neurochemical Sensor Interface

A. Neurochemical Cell

Sensitivity and selectivity of the sensor electrodes to neurochemicals play an important role in achieving good current resolution from the sensor interface circuit. The diamond-like carbon electrodes used in this work ensure stable detection of neurochemicals and exhibit low background current (I_{bg}) in electrochemical measurements [5]. The sensitivity and selectivity performance of the DLC electrodes is presented in [5], [6]. The impedance of the neurochemical cell also contributes to the performance of the current acquisition stage. The equivalent circuit and lumped impedance model of the neurochemical cell is presented in Fig. 2, which shows the interface between the neurochemical solution and the sensor electrodes. The reference electrode is usually designed to be inert to the reactions occurring within the cell and hence, its contribution to the cell impedance is negligible. The contribution of the solution resistances from the CE and WE interfaces (i.e. R_{sc} and R_{sw}) to the impedance of the counter electrode and working electrodes (Z_{CE} and Z_{WE}) respectively, are also known to be negligible [7]. Thus, the impedance of the working electrode (Z_{WE}) dominates the total impedance of the cell (Z_{cell}) since the oxidation and reduction reactions occur at the working electrode.

B. Neurochemical Signal Acquisition

The cell current from the sensor electrodes is processed within the sensor interface circuit as shown in Fig. 3. The circuit requirements are defined based on the need to provide a wide cell voltage range (V_{cell}) of 1.5V between WE and RE, while sensing a wide range of the electrochemically induced current (I_{cell}) that is flowing between CE and WE. In addition, the acquired current is digitized with an oscillator-based structure, which does not require analog sampling and benefits from technology scaling [8]. Finally, the digital output (D_{out}) from the sensor interface circuit can be utilized by closed loop brain machine interfaces for neurostimulation or prosthesis control.

The current acquisition (IA) stage is designed to provide stable V_{cell} between -0.7V to 0.8V potential window based

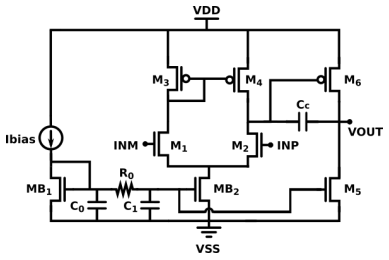

Fig. 4. Miller NMOS opamp with low-pass RC-filter.

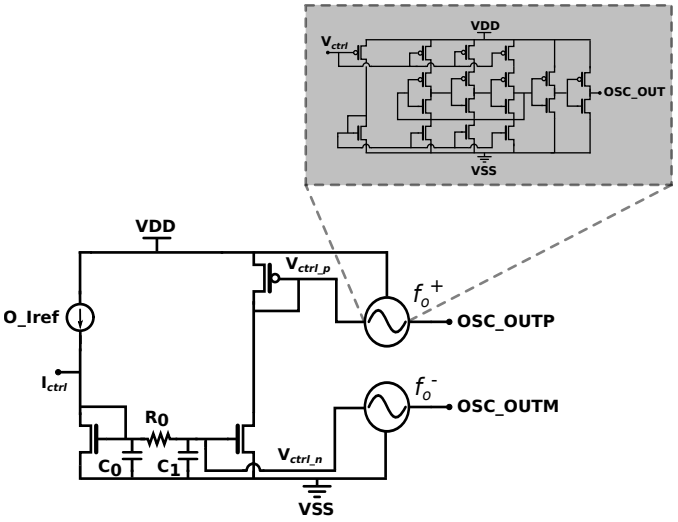

Fig. 5. Current controlled oscillator (CCO) schematic.

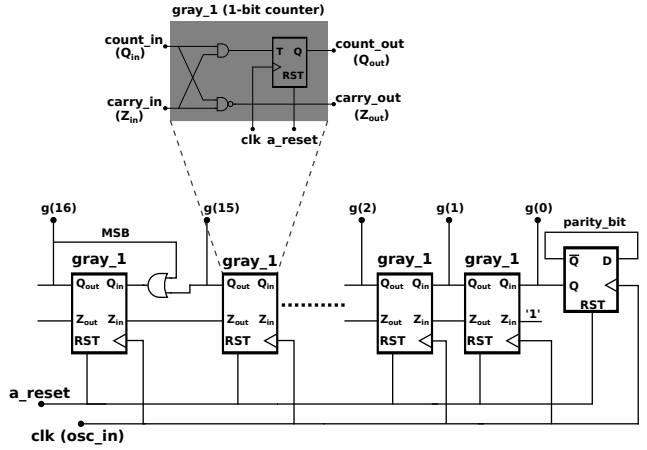

Fig. 6. 16-bit Gray code counter schematic.

on cyclic voltammetry sweep of the input voltage (V_{in}). The oxidation (I_{ox}) and reduction (I_{red}) current peaks from the neurochemical can be detected during the forward and reverse sweep of the input voltage as described in [8]. The potential window of 1.5V defines the input common-mode range (ICMR) and determines the minimum supply voltage of the operational amplifiers (opamp). The operational amplifiers, OP_1 and OP_2 are designed using the 2-stage Miller-compensated opamp architecture shown in Fig. 4. A simple low-pass RC-filter is implemented with R_0, C_0 and C_1 to limit high-frequency noise in the bias path of the opamp. Similar RC-filter is applied to the current acquisition and oscillator reference current paths (E_I_{ref}, O_I_{ref}). The opamp OP_1 together with OP_2 control V_{cell} by setting the voltage at the reference and working electrodes respectively as [8],

$$V_{cell} = V_{WE} - V_{RE} = V_{ref} - V_{in} \ . \tag{1}$$

Hence, the acquired cell current is defined by the ratio of the applied V_{cell} to the total impedance of the cell (Z_{cell}) as [8]:

$$I_{cell} = \frac{V_{cell}}{Z_{cell}} = \frac{V_{ref} - V_{in}}{Z_{cell}} \ . \tag{2}$$

The controllable bias current I_{ctrl} that flows into the CCO decreases or increases from the defined IA reference current E_I_{ref}, based on the acquired redox current I_{cell} from the neurochemical as [8]:

$$I_{ctrl} = E\_I_{ref} \mp I_{cell} \ . \tag{3}$$

Thus, E_I_{ref} can be re-configured to support a wide range of I_{cell} within $\pm 1.2\mu$A. This flexibility in the transimpedance structure makes the topology well-suited for neurochemical sensing applications.

The circuit implementation of the CCO that is used in the current-to-frequency (I-F) stage is presented in Fig. 5. The CCO is implemented with two current-starved ring oscillators. The CCO has an internal reference current (O_I_{ref}) that sets the operating center frequency of the oscillator. The frequency of the oscillator increases or decreases from the center frequency based on the control current I_{ctrl}. The dynamic range of the sensor interface circuit is determined by the frequency range of the CCO and the sampling rate defined in the current-to-digital (ID) stage [8]. The ID stage quantizes the pulses from the oscillator outputs with two 16-bit gray code counters, samples the counter codes with the sampling clock (F_s) and performs a difference operation on the sampled counter codes for noise-shaping. The schematic of the 16-bit gray code counter is presented in Fig. 6. Further details about the CCO-based analog-to-digital conversion is described in [8].

III. Measurement Results

The sensor interface circuit is fabricated in 65nm CMOS technology and Fig. 7(a) shows the die micrograph of the fabricated chip. The main processing blocks of the sensor interface circuit occupy an area of 0.059mm^2 (IA: 0.019mm^2, I-F: 0.005mm^2 and ID: 0.035mm^2). Cyclic voltammetric measurements were performed in a three-electrode setup with a Ag/AgCl reference electrode (Radiometer Analytical), a graphite rod as a counter electrode, and the DLC working electrode. The working electrode is designed with a 7nm DLC film thickness and an average surface roughness of 1.6nm. The surface roughness of the DLC electrode is presented in

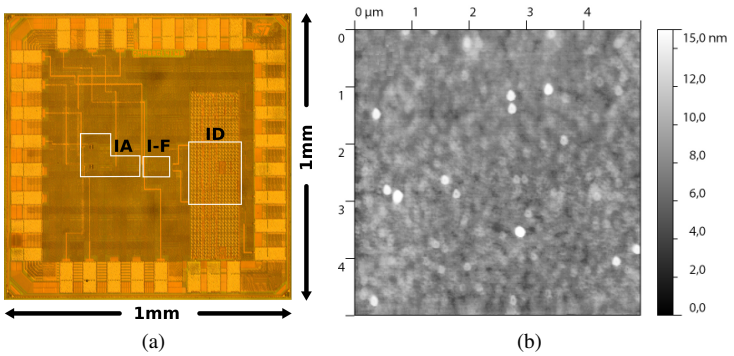

(a) (b)

Fig. 7. Die micrograph of the sensor interface chip in 65nm CMOS and topography map of the DLC electrode surface.

Fig. 7(b) as taken from an atomic force microscope (AFM). The DLC film was deposited with a filtered cathodic vacuum arc (FCVA) system on a 20nm Ti inter-layer on top of p-type Si (100). The dopamine concentrations used during the measurements were prepared by adding Dopamine hydrochloride (Sigma-Aldrich) to a phosphate-buffered solution (PBS) with pH value of 7.4.

Fig. 8 shows the input voltage that controls the sensor interface circuit and the cell voltage which defines the redox potential window for the CV measurements. The required input voltage range of 1.5V is applied and Fig. 8(a) shows that the sensor interface circuit supports the required input voltage range. Consequently, Fig. 8(b) shows that the required potential window of -0.7V to 0.8V is provided by the sensor interface circuit for the acquisition of the cell current.

The acquisition of the cell current from PBS solution is shown in Fig. 9(a). The acquired current from PBS serves as background current estimate (I_{bg}) when dopamine is added to the measurement setup. As a result, the background subtracted cell current ($I_{cell} - I_{bg}$) represents the change in current due to oxidation and reduction of dopamine. The CV measurement from the PBS solution is presented in Fig. 9(b). The upward progression of the CV measurement occurs due to the presence of oxygen in the neurochemical cell which depicts the environment in the brain. This demonstrates that using the DLC working electrode with the sensor interface circuit results in relatively stable detection of the background current also in the presence of oxygen.

Fig. 10 shows the digital output codes from the sensor interface circuit for I_{cell} range of $\pm 1.2\mu$A at sampling rate of 1KHz. The dynamic range of the digital output codes is 88.97dB (28098 LSBs), which corresponds to 14.5 bit digital code resolution from the sensor interface circuit and hence current sensitivity of 85.4pA/LSB. In addition, Fig. 11(a) and Fig. 11(b) show the digitized output from the sensor interface circuit when 500nMol of dopamine is added to the PBS solution and the oxidation and reduction peaks due to the presence of dopamine are also visible. Table I presents the summary of the measured performance of the sensor interface circuit and comparison with some prior work in similar application area.

IV. Conclusion

The detection of neurochemical concentration from the brain contributes to the implementation of fully-implantable closed-loop electronics for medical diagnosis and treatment of

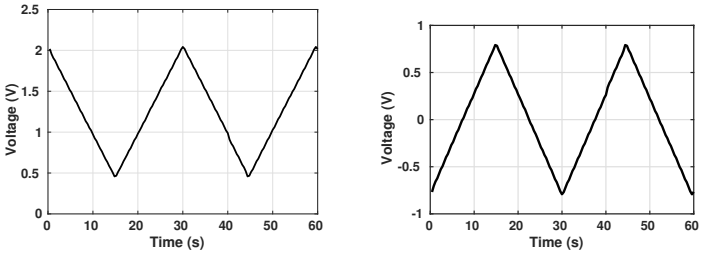

(a) V_{in} range = 1.5V (b) $V_{cell} = V_{ref} - V_{in}$

Fig. 8. Input control voltage at sweep rate of 100mV/s and the corresponding V_{cell} voltage between WE and RE.

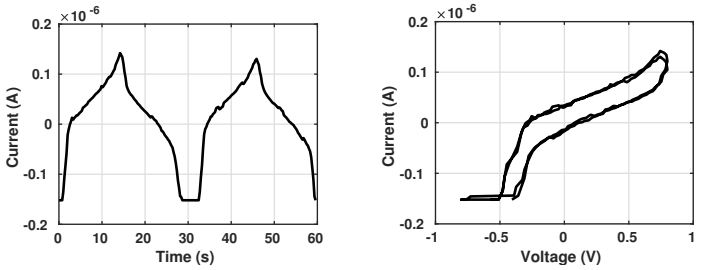

(a) I_{bg} from PBS solution (b) Cyclic voltammetry of I_{bg}

Fig. 9. Readout of I_{cell} (i.e. $I_{ctrl} - E\_I_{ref}$) from phosphate-buffered solution (PBS) which represents the background current I_{bg}.

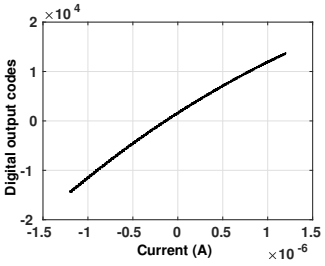

Fig. 10. Digital output codes (D_{out}) for I_{cell} range = $\pm 1.2\mu$A

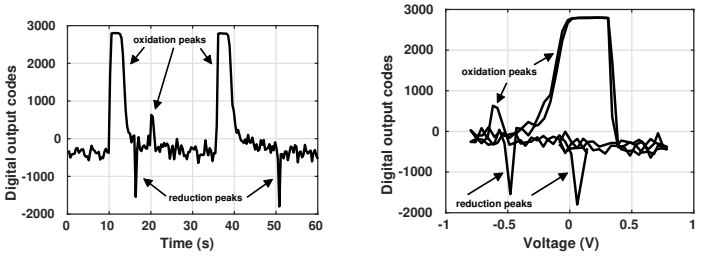

(a) D_{out} from 500nMol of dopamine (b) CV of the detected I_{cell} codes

Fig. 11. Digital output codes from PBS and 500nMol of dopamine showing the oxidation-reduction peaks and the corresponding oxidation-reduction potentials at which the redox peaks occur.

neurodegenerative diseases. This paper describes the design of a sensor interface circuit with wide input current range for neurochemical signal acquisition. The proposed circuit is fabricated in a 65nm CMOS process. Measured results show that the sensor interface circuit can detect dopamine concentration as low as 500nMol with novel diamond-like carbon sensor electrodes. In addition, the current resolution of the sensor interface circuit is 85.4pA within an input current range of $\pm 1.2\mu$A. Hence, the detected oxidation and reduction current peaks from the sensor interface circuit allows monitoring of the release times of neurochemicals in the brain and suitable stimulating potentials. The achieved current resolution and current range makes the sensor interface well-suited for neurochemical sensing applications.

TABLE I. PERFORMANCE COMPARISON

Design parameters	This work	JSSC 14, [9]	TBCAS 13, [10]
Technology (CMOS)	65**nm**	0.35μm	0.35μm
Input current range	$\pm 1.2\mu$**A**	$\pm 950n$A	$\pm 175n$A
Input current resolution	85.4p**A**	78pA	24pA
Control voltage range	1.5**V**	1.7V	1V
(CV potential window)	(−0.7**V,** 0.8**V**)	(−0.4V, 1.3V)	(−0.1V, 0.9V)
Sampling rate	1**kHz**	10kHz	1kHz
Dynamic range	88.97**dB**	80.8dB	-
Supply voltage	1.8**V**	2.5V	3.3V
Power consumption	49μ**W**	74.5μW	188μW
	18μ**W (IA stage)***	9.3μW (duty-cycled)**	

*power consumption of current acquisition stage, **average consumption in power-saving mode

ACKNOWLEDGMENT

The authors would like to thank Academy of Finland (#269196) for funding this research work.

REFERENCES

[1] J. M. Beaulieu and R. R. Gainetdinov, "The physiology, signaling, and pharmacology of dopamine receptors," *Pharmacological reviews*, vol. 63, no. 1, pp. 182–217, Mar 2011.

[2] R. K. Goyal and A. Chaudhury, "Structure activity relationship of synaptic and junctional neurotransmission," *Autonomic Neuroscience*, vol. 176, no. 1-2, pp. 11–31, 2013.

[3] M. Roham, D. Covey, D. Daberkow, E. Ramsson, C. Howard, B. Heidenreich, P. Garris, and P. Mohseni, "A Wireless IC for Time-Share Chemical and Electrical Neural Recording," *IEEE Journal of Solid-State Circuits*, vol. 44, no. 12, pp. 3645–3658, Dec 2009.

[4] K. H. Lee, C. D. Blaha, P. A. Garris, P. Mohseni, et al., "Evolution of Deep Brain Stimulation: Human Electrometer and Smart Devices Supporting the Next Generation of Therapy," *Neuromodulation: Technology at the Neural Interface*, vol. 12, no. 2, pp. 85–103, 2009.

[5] E. Kaivosoja, E. Berg, A. Rautiainen, T. Palomaki, J. Koskinen, M. Paulasto-Krockel, and T. Laurila, "Improving the function of dopamine electrodes with novel carbon materials," in *2013 35th Annual International Conference of the IEEE Engineering in Medicine and Biology Society (EMBC)*, July 2013, pp. 632–634.

[6] T. Laurila, V. Protopopova, S. Rhode, S. Sainio, T. Palomki, M. Moram, J. M. Feliu, and J. Koskinen, "New electrochemically improved tetrahedral amorphous carbon films for biological applications," *Diamond and Related Materials*, vol. 49, pp. 62–71, 2014.

[7] S. Martin, F. Gebara, T. Strong, and R. Brown, "A Fully Differential Potentiostat," *IEEE Sensors Journal*, vol. 9, no. 2, pp. 135–142, 2009.

[8] O. Olabode, M. Kosunen, and K. Halonen, "A current controlled oscillator based readout front-end for neurochemical sensing in 65nm cmos technology," in *2016 IEEE International Symposium on Circuits and Systems (ISCAS)*, May 2016, pp. 514–517.

[9] B. Bozorgzadeh, D. Covey, C. Howard, P. Garris, and P. Mohseni, "A neurochemical pattern generator SoC with switched-electrode management for single-chip electrical stimulation and 9.3 μW, 78 pA rms , 400 V/s fscv sensing," *IEEE J. Solid-State Circuits*, vol. 49, no. 4, pp. 881–895, 2014.

[10] M. H. Nazari, H. Mazhab-Jafari, L. Leng, A. Guenther, and R. Genov, "Cmos neurotransmitter microarray: 96-channel integrated potentiostat with on-die microsensors," *IEEE Transactions on Biomedical Circuits and Systems*, vol. 7, no. 3, pp. 338–348, June 2013.